

Novel Asymmetric Synthesis of Atropisomeric 6-Aryl Pyrazinones via an Unusual Chirality Transfer Process

John Tulinsky,¹ B. Vernon Cheney, Stephen A. Mizsak, William Watt, Fusan Han, Lester A. Dolak, Thomas Judge, and Ronald B. Gammill*[†]

Structural, Analytical and Medicinal Chemistry, Pharmacia & Upjohn, Inc., Kalamazoo, Michigan 49001-0199

Received June 18, 1998

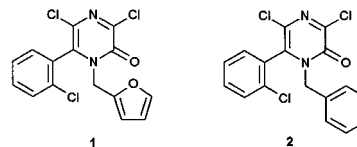
Cyclization of (*S,S*)- α -(1-phenylethyl)amino- α -(2-iodophenyl)acetonitrile with (COCl)₂ in toluene or chlorobenzene afforded the atropisomeric pyrazinone (*aS,S*) 6-(2- α -iodophenyl)-3,5-dichloro-1-(1-phenylethyl)-2(1*H*)-pyrazinone in 57% yield. With smaller *ortho* substituents (F, Cl, CH₃, CF₃, OCH₃) on the aromatic ring, mixtures of atropisomers were obtained from the cyclization reaction. All of the individual atropisomers prepared were stable at room temperature. All but the *o*-fluoro-substituted atropisomers were stable at elevated temperatures. This paper describes a stereoselective synthesis of pyrazinones and suggests a mechanism for formation via an interesting transfer of chirality.

Introduction

Chiral atropisomeric compounds are of considerable interest due to their presence in a number of biologically active natural and synthetic products and their utility as directing groups in asymmetric synthesis.² The interesting physical, chemical, and biological properties of these compounds is reflected and to a vast extent controlled by the relative conformation of the two aromatic rings.^{2,3} In principle, heteroaryl-aryl atropisomers^{3b} offer certain opportunities for structural and physical change that are not available in the more classical biphenyl systems. For example, heteroatoms provide an opportunity to probe a wide variety of geometric and electronic situations unavailable in the biphenyl system.³ Despite many recent advances in the asymmetric synthesis of chiral biphenyl and heteroaryl-aryl atropisomeric com-

pounds, efficient and expedient methods of synthesis remain the gatekeepers for the delineation of new and interesting chemical and biological properties of such molecules.

Pyrazinones **1** and **2** are recently discovered ligands at Pharmacia & Upjohn that bind to a new site on the GABA_A/chloride ionophore complex.^{6a,b} In the ¹H NMR spectra of pyrazinones **1** and **2**, the methylene hydrogens



(3) (a) For reviews and papers discussing axially chiral heteroaromatics, see: Gallo, R.; Roussel, C.; Berg, U. In *Advances in Heterocyclic Chemistry*; Katritzky, A. R., Ed.; Academic Press: San Diego, 1988; Vol. 43, p 173. Roussel, C.; Adjimi, M.; Chemlal, C.; Djafri, A. *J. Org. Chem.* **1988**, *53*, 5076. Dogan, I.; Pustet, N.; Mannschreck, A. *J. Chem. Soc., Perkin Trans. 2* **1993**, 1557. (b) For specific examples and leading references of heterocyclic systems, see: for *N*-aryl-4-thiazoline-2-thiones, Roussel, C.; Djafri, A. *New J. Chem.* **1986**, *10*, 399. For the anaesthetic ketamine, the tranquilizer etazqualone, and the anthelmintic praziquantel: Mannschreck, A.; Koller, H.; Wernick, R.; *Kontakte, Darmstadt* **1985**, *1*, 40. For examples of flavins: Shinkai, H.; Nakao, H.; Kuwahara, I.; Miyamoto, M.; Yamaguchi, T.; Manabe, O. *J. Chem. Soc., Perkin Trans. 1* **1988**, 313. For *N*-aryl-4-pyridones: Mintas, M.; Orhanovic, Z.; Jakopcic, K.; Koller, H.; Stuhler, G.; Mannschreck, A. *Tetrahedron* **1985**, *41*, 229. For *N*-arylpyrroles: Vorkapic-Furac, J.; Mintas, M.; Burgemeister, R.; Mannschreck, A. *J. Chem. Soc., Perkin Trans. 2* **1989**, 713. For the anticonvulsant and hypnotic methaqualone: Mannschreck, A.; Koller, H.; Stuhler, G.; Davies, M. A.; Traber, J. *Eur. J. Med. Chem.* **1984**, *19*, 381. For *N*-aryl-2(1*H*)-quinolones and *N*-aryl-6(5*H*)-phenanthridones: Mintas, M.; Mihaljevic, N.; Koller, H.; Schuster, D.; Mannschreck, A. *J. Chem. Soc., Perkin Trans. 2* **1990**, 619. (c) For a recent report on the atroposelective thermal reactions of axially twisted amides and imides, see: Curran, D. P.; Qi, H.; Geib, S. J.; DeMello, N. C. *J. Am. Chem. Soc.* **1994**, *116*, 3131.

(4) For references leading to general discussions, see: Wainer, I. W. *Drug Stereochemistry: Analytical Methods and Pharmacology*, M. Dekker, Inc.: New York, 1993. Ariens, E. J. *Trends Pharm. Sci.* **1993**, *14*, 68. Williams, K. M. *Adv. Pharmacol.* **1991**, *22*, 57. Ariens, E. J. *Med. Res. Rev.* **1986**, *6*, 451. Lam, Y. W. *Pharmacotherapy* **1988**, *8*, 147. For examples of enantiomers, see: Froimowitz, M.; Pick, C. G.; Pasternak, G. W. *J. Med. Chem.* **1992**, *35*, 1521 and references therein (CNS related). Macor, J. E.; Blake, J.; Fox, C. B.; Johnson, C.; Koe, B. K.; Level, L. A.; Morrone, J. M.; Ryan, K.; Schmidt, A. W.; Schulz, D. W.; Zorn, S. H. *J. Med. Chem.* **1992**, *35*, 4503. Ariens, E. J. *Trends Pharm. Sci.* **1986**, 200. Hoyer, D. *Trends Pharm. Sci.* **1986**, 227. Lehmann, P. A. *Trends Pharm. Sci.* **1986**, 281.

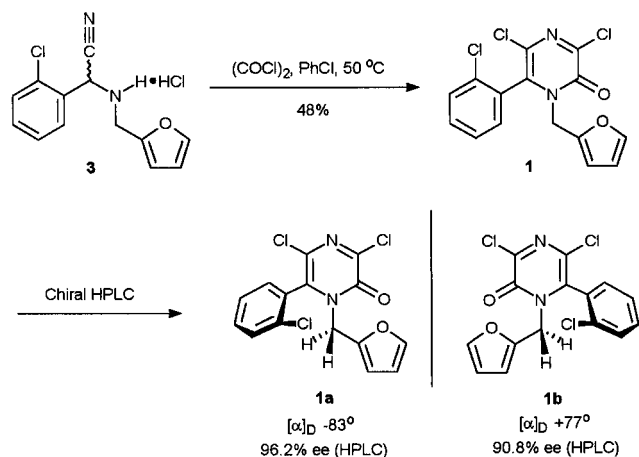
(5) Colebrook, L. D.; Giles, H. G.; *Can. J. Chem.* **1975**, *53*, 3431. Bringmann, G.; Hartung, T.; Gobel, L.; Schupp, O.; Peters, K.; von Schnering, H. G. *Liebigs Ann. Chem.* **1992**, 769.

[†] Current Address: Central Research Division, Pfizer, Inc., Groton, CT 06340.

(1) Postdoctoral Research Scientist 1993–95. Current address: Discovery Research, Cell Therapeutics, Inc., 201 Elliott Ave W., Seattle, WA 98119.

(2) The term atropisomerism refers to optical isomerism resulting from restricted rotation about a single bond. Biphenyls represent but one example of this type of isomerism. (a) For a general discussion of atropisomeric compounds, see: Oki, M. In *Topics in Stereochemistry*; Allinger, N. L., Eliel, E. L., Wilen, S. H., Eds.; John Wiley and Sons: New York, 1983. Eliel, E. L. *Stereochemistry of Carbon Compounds*; McGraw-Hill: New York, 1995. For recent asymmetric syntheses of atropisomeric compounds, see: Lipshutz, B. H.; Liu, Z.; Kayer, F. *Tetrahedron Lett.* **1994**, 5567. Feldman, K. S.; Ensel, S. M.; Minard, R. D. *J. Am. Chem. Soc.* **1994**, *116*, 1742. Nelson, T. D.; Meyers, A. I. *J. Org. Chem.* **1994**, *59*, 2577, 2655. Suzuki, T.; Hotta, H.; Hattori, T.; Miyano, S. *Chemistry Lett.* **1990**, 807. For a fairly recent review on the subject of biaryl synthesis, see: Bringmann, G.; Walter, R.; Weirich, R. *Angew. Chem., Int. Ed. Engl.* **1990**, *29*, 977. (b) For leading references regarding the biological properties of atropisomeric compounds, see: Govindachari, T.; Nagarajan, K.; Parthasarathy, P. C.; Rajagopalan, T. G.; Desai, H. K.; Kartha, G.; Chen, S. K.; Nakanishi, K. *J. Chem. Soc., Perkin Trans. 1* **1974**, 1413. Bringmann, G. In *The Alkaloids*; Academic Press: New York, 1986; Vol. 29, p 141. Huang, L.; Si, Y.-K.; Snakzke, G.; Zheng, D.-K.; Zhou, J. *Collect. Czech. Chem. Commun.* **1988**, *53*, 2664. Uchida, I.; Ezaki, M.; Shigematsu, N.; Hashimoto, M. *J. Org. Chem.* **1985**, *50*, 1341. Kannan, R.; Williams, D. H. *J. Org. Chem.* **1987**, *52*, 5435. Kupchan, S. M.; Britton, R. W.; Ziegler, M. F.; Gilmore, C. J.; Restivo, R. J.; Bryan, R. F. *J. Am. Chem. Soc.* **1973**, *95*, 1335. Tomioka, K.; Ishiguro, T.; Koga, K. *Tetrahedron Lett.* **1980**, 2973. (c) For an excellent discussion on the use of stereochemistry as a probe of pharmacological receptors, see: Casy, A. F. *The Steric Factor in Medicinal Chemistry. Dissymmetric Probes of Pharmacological Receptors*; Plenum Press: New York, 1993.

Scheme 1



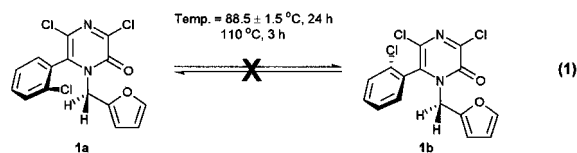
at N-1 are nonequivalent. This structural information suggested that these pyrazinones might exist as atropisomers due to restricted rotation about the heteroaryl carbon-carbon bond.⁵ This observation, coupled with the interesting biological activity, presented an opportunity to investigate both the chemistry and biology of the 6-arylpyrazinones, a new class of atropisomers.

In this paper, we confirm the atropisomeric nature of 6-arylpyrazinones and establish the absolute stereochemistry of representatives from this class of compounds. Furthermore, we discuss a simple and highly efficient asymmetric synthesis and present a mechanistic rationale for an unusual chirality transfer process.

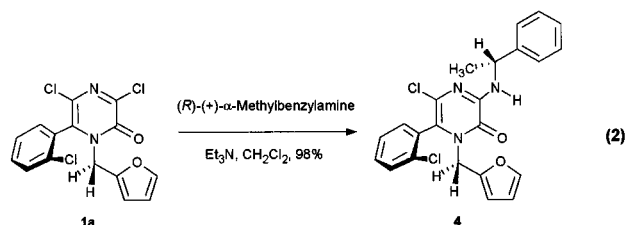
Results and Discussion

Pyrazinones **1** and **2** were readily synthesized in two steps from commercially available starting materials (Scheme 1). Strecker reaction of an amine hydrochloride, an *ortho*-substituted benzaldehyde, and sodium cyanide in aqueous methanol afforded the desired racemic aminonitrile **3**. Treatment of that aminonitrile hydrochloride with an excess of oxalyl chloride in chlorobenzene or toluene at 50 °C then provided pyrazinone **1**.⁸ Pyrazinones **1** and **2** were readily resolved into their enantiomeric counterparts via analytical HPLC using a chiral stationary phase (Scheme 1).⁹ We established that the chiral axis of the pyrazinone was thermally stable in the following manner. Toluene solutions of enantiomer **1a** were heated, and aliquots were removed periodically and analyzed by HPLC. After 21 h at 90 °C and 3 h at 110

°C, **1a** remained homogeneous by chiral HPLC analysis (eq 1). These experiments convincingly demonstrated



that pyrazinones such as **1** could be resolved into their enantiomeric pairs and that those enantiomers are configurationally stable at 100 °C for several hours. To assign the absolute stereochemistry of enantiomers **1a** and **1b**, the earlier eluting enantiomer (**1a**; $[\alpha]_D -83^\circ$) was coupled with (*R*)-(+)- α -methylbenzylamine to yield the 3-amino-substituted pyrazinone **4** (eq 2) in 98% yield.



The absolute configuration of **4** was established by single-crystal X-ray analysis (see Supporting Information) and proved to be (*aS*) about the aryl-heteroaryl bond.¹⁰ To continue our investigation into the stereochemical aspects and, specifically, the possibility of devising an asymmetric synthesis of these compounds, we elected to introduce an asymmetric center into our starting aminonitrile via the introduction of an α -methylbenzylamine group. We hoped that introduction of an asymmetric center would provide us with some insight into the reaction pathway and as a minimum provide us with easier analysis and isolation of reaction products (diastereomers vs enantiomers).

Reaction of (*R*)- or (*S*)- α -methylbenzylamine hydrochloride, an aryl aldehyde, and sodium cyanide (Strecker reaction, see Scheme 2) in aqueous methanol afforded the corresponding aminonitriles **5** and **7** in quite satisfactory yield with moderate diastereoselectivity (Table 1).¹¹ In general, the major diastereomer resulting from the Strecker reaction (**5** or **7**) could be purified to homogeneity through recrystallization of the corresponding HCl salts. However, in several cases (**6b**, **8b**, **5g**, **7g**, **7j**, and **8k**), diastereomerically pure aminonitriles were more difficult to obtain and were used as enriched mixtures (see Table 1). Cyclization of diastereomerically pure **5a** and **7a**, derived from *o*-iodobenzaldehyde with an excess

(6) (a) Tulinsky, J.; Mizsak, S. A.; Watt, W.; Dolak, L. A.; Judge, T. M.; Gammill, R. B. *Tetrahedron Lett.* **1995**, *36*, 2017. Im, H. K.; Im, W. B.; Judge, T. M.; Gammill, R. B.; Hamilton, B. J.; Carter, D. B. *Mol. Pharmacol.* **1993**, *44*, 468. In light of their dramatic and direct influence on chloride flux, it is likely that pyrazinones bind at a site within the channel domain of the complex. In contrast to barbiturates, which also modulate the GABA_A complex in an allosteric fashion, concentrations of the pyrazinones greater than that which elicits the maximum effect on the chloride channel have no further effect on chloride flux. Thus, the pyrazinones potentially offer a template in which the pharmacological toxicity associated with barbiturates may be reduced. (b) Tulinsky, J.; Gammill, R. B. *Curr. Med. Chem.* **1994**, *1*, 226. Gammill, R. B.; Carter, D. *Annu. Rep. Med. Chem.* **1994**, Chapter 5.

(7) All new compounds had physical and analytical properties (¹H and ¹³C NMR, IR, UV, MS, HRMS, and combustion analysis) consistent with their assigned structures.

(8) Vekemans, J.; Pollers-Wieers, C.; Hoornaert, G. *J. Heterocycl. Chem.* **1983**, *20*, 919.

(9) Separation by chiral HPLC was achieved on a (*R,R*) Whelk-01 column (0.46 × 25 cm); elution with 30% 2-propanol in hexane, 1.5 mL/min, UV monitor at 345 nm.

(10) Further information regarding the crystal structure of **4** will be published elsewhere. A ball-and-stick drawing of **4** is provided in the Supporting Information.

(11) (a) Stout, D. M.; Black, L. A.; Matier, W. L. *J. Org. Chem.* **1993**, *48*, 5369. A single recrystallization of the hydrochloride salt of the aminonitrile was generally sufficient to provide the pure (*R,R*) or (*S,S*) diastereomer. The absolute stereochemistry of the aminonitrile was established via single-crystal X-ray crystallography. A representative description of the Strecker reaction can be found in the Experimental Section. (b) In the stereochemical designation of the aminonitriles, the first center listed relates to the α -methylbenzyl center and the second to the nitrile-bearing carbon. In the pyrazinones, the first center designated relates to the chiral axis and the second to the α -methylbenzyl center. The prefix *a* denotes axial chirality. This can lead to confusion in the interpretation of the data if not recognized. (b) For a leading reference on the epimerization of related aminonitriles, see: Subramanian, P. K.; Woodard, R. W. *Synth. Commun.* **1986**, *16*, 337. Patel, M. S.; Worsley, M. *Can. J. Chem.* **1970**, *48*, 1881.

Scheme 2

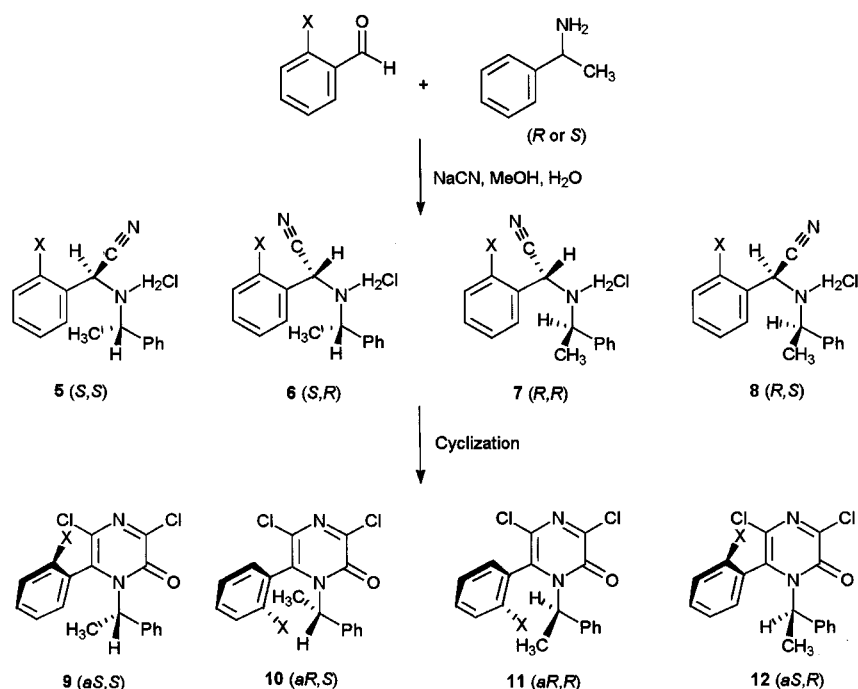
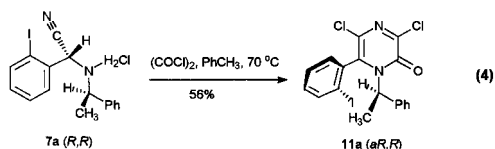
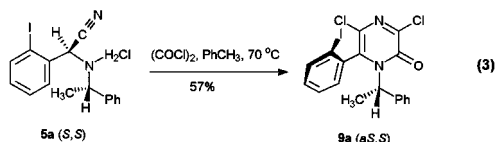


Table 1. Data for Aminonitrile Structures 5–8

entry	Ar	aminonitrile ^a	% yield
a	2-iodophenyl	5	81
a	2-iodophenyl	7	54
b	2-bromophenyl	5	56
b	2-bromophenyl	6	15 (90% de)
b	2-bromophenyl	7	52
b	2-bromophenyl	8	14 (88% de)
c	2-chlorophenyl	7	52
d	2-fluorophenyl	5	60
d	2-fluorophenyl	7	62
e	2-methylphenyl	5	54
e	2-methylphenyl	7	40
f	2-trifluoromethyl	7	48
g	2-methoxyphenyl	5	27 (88% de)
g	2-methoxyphenyl	7	23 (92% de)
h	2,3-difluorophenyl	5	46
i	3-methylphenyl	7	33
j	1-naphthyl	7	54 (93% de)
k	1-thienyl	5	48 (98% de)
k	1-thienyl	7	51
k	1-thienyl	8	4 (95% de)

^a All aminonitriles were homogeneous by ¹H NMR (300 MHz) unless otherwise stated.

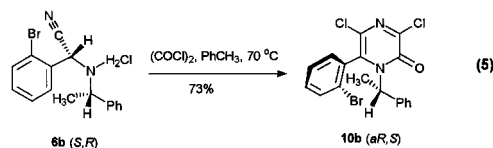
of oxalyl chloride in chlorobenzene at 70 °C for 14 h, provided pyrazinones (*aS,S*) **9a** and (*aR,R*) **11a** respectively, in 57% and 56% yields (eqs 3 and 4). Conducting



the reaction in a sealed tube (see Experimental Section) gave a slight improvement in the yield. The relative and absolute stereochemistry of the (*aR,R*) pyrazinone **11a**

was established by X-ray crystallography (Supporting Information). The diastereomer of a mixture of aminonitrile diastereomers (**7a** and **8a**). An X-ray of pyrazinone **12a** was also obtained (Supporting Information), providing further structural information about axially chiral pyrazinones.¹⁴ These initial experiments with aminonitrile substrates containing a chiral auxiliary established that an efficient method for asymmetric synthesis of these pyrazinones was possible.

Cyclization of the diastereomerically pure (*S,S*) and (*R,R*) aminonitriles **5b** and **7b** derived from *o*-bromobenzaldehyde likewise proceeded with high stereoselectivity (see Table 2) to provide diastereomerically pure pyrazinones (*aS,S*) **9b** and (*aR,R*) **11b**. We suspected from the above results that the nitrile-bearing carbon in the aminonitrile was transferring its configuration to the chiral axis in the pyrazinone. Indeed, cyclization of the (*S,R*) bromoaminonitrile **6b** (90% de; eq 5) afforded the



corresponding (*aR,S*) pyrazinone **10b**

(12) Charton, M. *J. Org. Chem.* **1977**, *42*, 2528. Roussel, C.; Ayada, D. *Nouv. J. Chim.* **1986**, *10*, 399.

(13) In the case of biphenyls, steric size of the *ortho* substituents as measured by barriers to rotation match increased/decreased selectivity in pyrazinone synthesis. For examples in the biphenyl series, see: Ling, C. H. K.; Harris, M. H. *J. Chem. Soc.* **1964**, 825. Oki, M.; Yamamoto, G. *Bull. Chem. Soc. Jpn.* **1971**, *44*, 266. Adams, R. *Rec. Prog. Chem.* **1949**, 91.

(14) The (*aS,R*) pyrazinone diastereomer **12a** was obtained from the cyclization of a 4:1 mixture of the aminonitriles **8a** and **7a**. That reaction afforded a 4:1 mixture of the (*aS,R*) and (*aR,R*) pyrazinones **12a** and **11a** in 24% yield. Column chromatography was sufficient to provide each diastereomer as a pure compound. The absolute stereochemistry of the (*aR,R*) and (*aS,R*) diastereomers was confirmed through single-crystal X-ray crystallography. Full details of the X-ray data for **11a** and **12a** will be published elsewhere. Ball-and-stick drawings of **11a** and **12a** are provided in the Supporting Information.

Table 2. Data for Atropisomeric Pyrazinone Structures 9–12

entry	X or 6-aryl	aminonitrile (de) ^a	pyrazinone (ratio) ^a	% yield ^b
a	I	5	9	57 (60)
a	I	7	11	56 (62)
b	Br	5	9	64 (55)
b	Br	6 (90%)	10/9 (8:1)	73
b	Br	7	11	68 (54)
b	Br	8 (88%)	12/11 (18:1)	43
c	Cl	7	11/12 (1.4:1)	67
d	F	5	9/10 (1:1)	70
d	F	7	11/12 (1:1)	62
e	CH ₃	5	9/10 (4:1)	71 (72)
e	CH ₃	7	11/12 (4:1)	28 (73)
f	CF ₃	7	11/12 (3.4:1)	33
g	OCH ₃	5 (88%)	9/10 (1.2:1)	61
g	OCH ₃	7 (92%)	11/12 (1:1)	78
h	2,3-F	5	9/10 (1:1)	68
i	3-CH ₃	7	11/12 (1:1)	59
j	1-naphthyl	7	11/12 (1:1)	45
k	1-thienyl	5	9	48
k	1-thienyl	7	11	24

^a de's and product ratios were determined by ¹H NMR (300 MHz). If no de or ratio is listed, product was homogeneous by ¹H NMR. Aminonitriles were epimeric at the nitrile-bearing carbon. ^b Yields in parentheses are for reactions carried out in a sealed tube vs a reaction vessel under a positive nitrogen pressure.

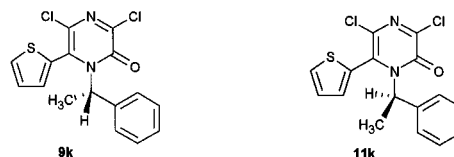
(78% de) in 73% yield, further supporting our notion that the configuration about the chiral axis was indeed determined by the configuration at the nitrile-bearing carbon in the acyclic precursor and not by the chiral auxiliary.

To continue to probe the mechanistic aspects of the cyclization, we investigated the influence of the *ortho* aryl substituent on the stereochemical course of the reaction. As illustrated in Table 2, cyclization of the diastereomerically pure (*R,R*) aminonitrile **7c** containing an *o*-Cl substituent afforded a 1.4:1 mixture of pyrazinones (*aR,R*) **11c** and (*aS,R*) **12c**. With the smaller *o*-F substituent (*S,S*) **5d**, cyclization afforded an equimolar mixture of pyrazinones (*aS,S*) **9d** and (*aR,S*) **10d**. This was also true for the 2,3-difluoro aminonitrile example **5h** (obtained diastereomerically pure from a single recrystallization), establishing the absence of a buttressing effect in the case of *o*-fluoro substitution.¹² Cyclization of the *o*-CH₃ and *o*-CF₃ aminonitriles (*R,R*) **7e** and (*R,R*) **7f** afforded the corresponding pyrazinones in 4:1 (**11e/12e**) and 3.4:1 (**11f/12f**) ratios, respectively. Aminonitrile **5g**, with an *o*-OCH₃ substituent, afforded an equimolar mixture of pyrazinones **9g** and **10g**. Cyclization of the naphthyl aminonitrile **7j** also afforded a mixture of diastereomeric pyrazinones (**11j** and **12j**). Last, cyclization of the *m*-methylaryl aminonitrile **7i** gave an equimolar mixture of pyrazinones **11i** and **12i**, supporting the obvious in that the major influence on the stereochemical outcome of the reaction was indeed the *ortho* substituent and that the influence was steric in nature. The above trends are also consistent with those seen in the biphenyl series.¹³

To examine the possibility that racemization of the pyrazinones was occurring after their formation, the *o*-fluoro-substituted pyrazinones were examined more closely. Resolution of **11d** and **12d** was readily achieved via preparative HPLC. A solution of **11d** in toluene-*d*₈ was heated at 70–75 °C for 20 h, conditions that *thermally* mimic the cyclization protocol. The ¹H NMR of the solution after 20 h at 70–75 °C showed a 7/3

mixture of **11d/12d**, indicating that partial racemization had occurred. When similar experiments were carried out with pyrazinones **11b**, **11c**, **11e**, and **11g**, no evidence of racemization about the asymmetric axis was observed by NMR. From that data, we concluded that although the configuration about the asymmetric axis is determined by the configuration at the nitrile-bearing carbon, the selectivity is related to the steric bulk of the *ortho* substituent. Racemization of the pyrazinone after formation plays little or no role in determining the final product ratio in all but the *o*-F case.

All of the 6-aryl pyrazinones studied in which there is an *ortho* substituent on the aromatic ring are conformationally locked at ambient temperature, including the *o*-fluoro-substituted case. To help further define the limits of conformational stability, we replaced the 6-aryl group with an aromatic heterocycle, thiophene. The required aminonitriles **5k** and **7k** were prepared using the normal Strecker protocol and when submitted to the cyclization conditions afforded the corresponding 6-thienyl pyrazinones. However, unlike the *ortho*-substituted aryl cases, each of the diastereomeric thiophene aminonitriles **5k** and **7k** gave a single pyrazinone product by ¹H NMR, **9k** and **11k**, respectively, indicating free rotation about

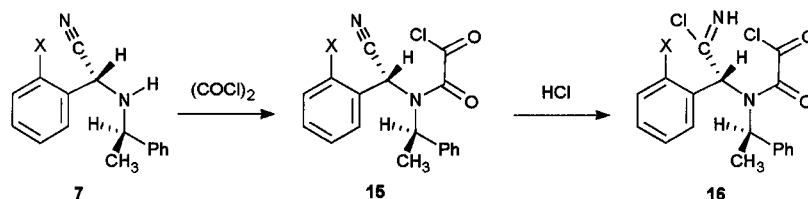
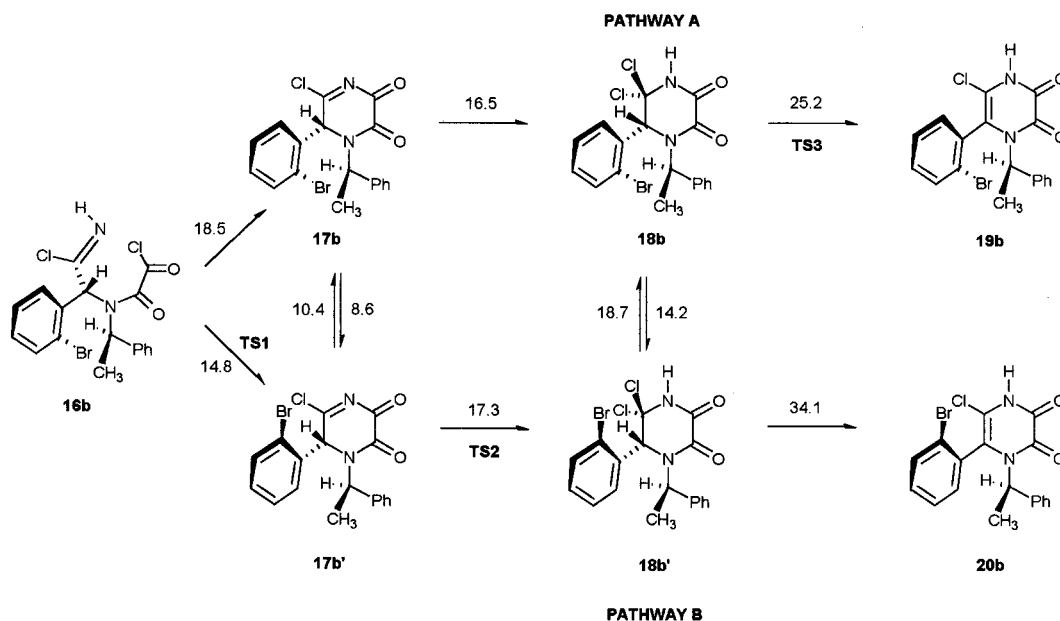


the aryl-heteroaryl axis in this case. Interestingly, the thienyl-substituted pyrazinones exhibit ¹H NMR characteristics at ambient temperature indicating hindered rotation on the NMR time scale. The H-1 proton signal corresponding to the methine of the α -benzyl substituent was broadened rather than existing as a sharp quartet.

As the temperature was increased, the resolution of the methine improved and the sharpness of the quartet improved. At lower temperatures, the methine signal broadened as expected. The lowest temperature examined was 5 °C, and at that temperature, the signals have not decoalesced into those of separate atropisomers. While qualitative in nature, these results imply that the thienyl-substituted pyrazinones are a borderline case in which rotation about the biaryl bond is slow on the NMR time scale but sufficiently unhindered to prevent physical resolution of the individual atropisomers.

Reactions to form the pyrazinones from the aminoacetonitrile hydrochloride compounds were carried out with excess oxalyl chloride using either chlorobenzene or toluene as solvent. Saturation of the system with HCl is essential for complete reaction. Intermediates produced during the course of the reaction were too short-lived to be isolated or characterized. For this reason, we employed computational methods as a means of gaining insight into the involvement of HCl and the mechanistic basis for stereoselectivity. Because the low dielectric constant of the solvent rules out ionic mechanisms, a series of reactions were investigated in which molecular HCl serves as a catalyst. On the basis of the results of those calculations, which are discussed in some detail hereafter, we propose the following mechanism to explain the stereospecific pyrazinone formation and chirality transfer. As shown in Scheme 3, initial acylation of aminonitrile **7** with oxalyl chloride provides the oxoamide inter-

Scheme 3. Proposed Mechanism for Pinner Salt Formation

Scheme 4^a

^a Barriers in kcal mol⁻¹ are indicated by numbers on the arrows for the transition.

mediate **15**. Addition of HCl across the nitrile triple bond then forms Pinner salt **16**,¹⁶ which induces two distinct modes of cyclization leading to either **17b** or **17b'** in the case where X is bromine, as illustrated in Scheme 4. Addition of HCl to either **17b** or **17b'** is believed to give rise to the corresponding *gem*-dichloro intermediates **18b** and **18b'**.¹⁷ Elimination of HCl from those intermediates then yields diones **19b** and/or **20b**. Thereafter, reaction of the diones with oxalyl chloride yields the final products. To gain further insight into stereochemical control of the reaction, it is necessary to examine the dynamics between the intermediates that fall on the reaction coordinate from **16b** to **19b** or **20b**.

By means of AM1 molecular orbital calculations, we examined the cyclization step involving the conversion of **16b** to **17b/17b'**, the addition of HCl to **17b/17b'** to

yield intermediate **18b/18b'**, and finally the process whereby HCl is lost from **18b/18b'** to yield **19b** and/or **20b**. Although this method yields highly approximate values of potential-energy barriers, trends in barrier height often provide useful insights into the underlying mechanisms in a series of chemical reactions. In the initial series of calculations, we wished to determine which step exerts the greatest control over the final stereochemical outcome.

Scans of the torsional angle θ governing rotation about the biaryl bond in **19b** (Figure 1) revealed barriers exceeding 30 kcal mol⁻¹ in the potential-energy curve, $V(\theta)$. In light of these high values, atropisomerism is clearly established in this intermediate leading to **11b**, and the final step involving the reaction of **19b** with oxalyl chloride need not be further considered. Scheme 4 illustrates two reaction pathways and gives the calculated barriers for transitions leading to either **19b** or **20b**. The unaided cyclization (**16** → **17**), addition (**17** → **18**), and elimination (**18** → **19**) reactions involve four-electron Hückel transition states with extremely high barriers.¹⁸ In contrast, the transition-state complexes shown in Figure 2 are each stabilized by a catalytic HCl molecule in a six-electron pericyclic process. The magnitude of the reaction barriers shown in Scheme 4 gives qualitative insight as to which step controls the stereochemistry.

(15) NOE experiments revealed a characteristic interaction in each diastereomer between the *o*-hydrogen of the aryl ring and the methine or methyl hydrogens of the *l*-methylbenzyl group. This observation proved to be a convenient means of assigning the stereochemistry of the diastereomeric pyrazinones.

(16) A simple model for Pinner salt formation using HCl attack on acetonitrile yields a very high barrier (56.6 kcal mol⁻¹). A much lower barrier (26.3 kcal mol⁻¹) is found using a second HCl molecule as catalyst. The calculations suggest that the reaction may avoid the high entropic cost of a tertiary collision by proceeding through two binary steps where an acetonitrile⋯HCl complex serves as intermediate. In any case, Pinner salt formation is suggested to be the rate-determining step of the reaction on the basis of simulation of the kinetics of the system (see Supporting Information) using the CHEMKIN II program (Kee, R. J.; Rupley, F. M.; Miller, J. A. *CHEMKIN II: A Fortran Package for the Analysis of Gas Phase Chemical Kinetics*; Sandia National Laboratories, Livermore, CA, report SAND 89-8009). Although CHEMKIN II has been designed for gas-phase kinetics, it may be appropriately used in constant-temperature studies with rate constants determined for condensed fluids.

(17) The calculated barriers exceed 50 kcal mol⁻¹ for HCl attack on **17b/17b'** to give **19b/19b'** in a direct tautomerization reaction, whereas those for HCl addition to **17b/17b'** are less than 20 kcal mol⁻¹. As a result, the low-energy pathways lead to production of the *gem* dichloro intermediates **18b/18b'**.

(18) Simons, J. *Energetic Principles of Chemical Reactions*; Jones and Bartlett: Boston, 1983; pp 65–68.

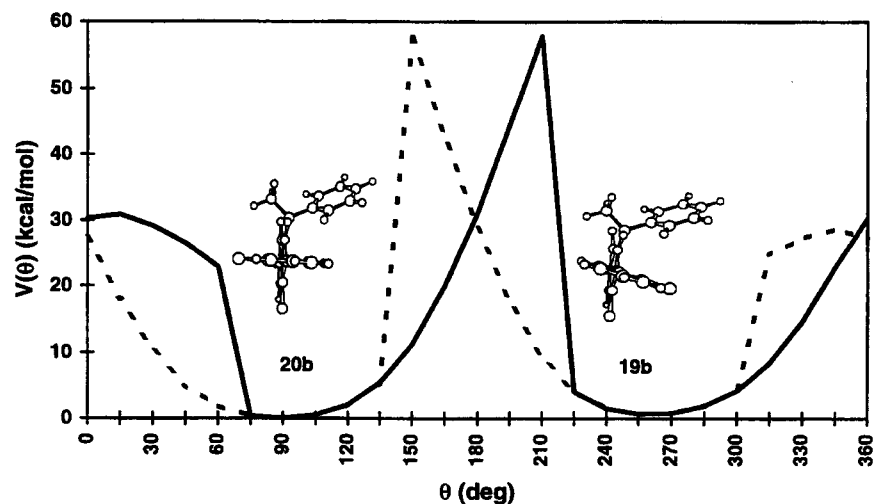


Figure 1. Rotation about the biaryl bond of **19b** leads to notable distortion of the pyrazino ring as Br sweeps past the α -methylbenzyl and chlorine substituents when θ is near 0° and 180° , respectively. A sharp drop in energy occurs as the system relaxes when the bulky *ortho* substituents on each ring push beyond one another. The shape of the barrier is dependent upon the direction of rotation, as shown by the solid (increasing θ) and dashed (decreasing θ) curves.

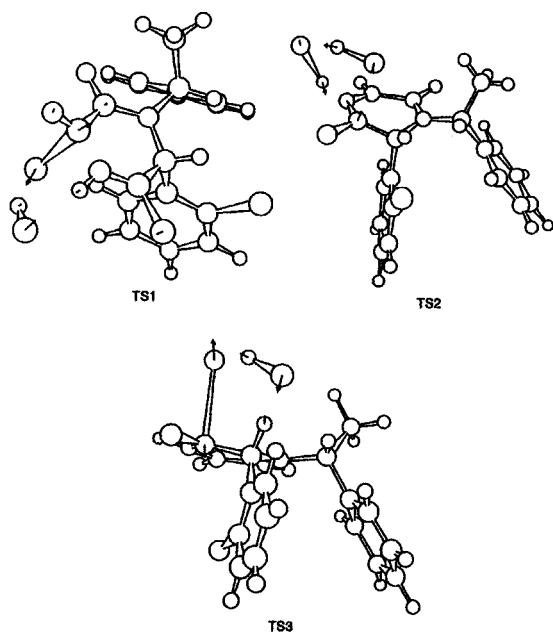


Figure 2. Transition-state complexes in the favored pathways for the reactions: **TS1** corresponds to the cyclization step **16b** \rightarrow **17b**; **TS2** is associated with the HCl-addition step **17b** \rightarrow **18b**; and **TS3** corresponds to the HCl-elimination step **18b** \rightarrow **19b**. Each reaction is catalyzed by HCl. Arrows represent motion of atoms along the reaction coordinate leading to products.

Values of the barriers are $14.8 \text{ kcal mol}^{-1}$ for cyclization of **16b**, $17.3 \text{ kcal mol}^{-1}$ for HCl addition to **17b'**, and $34.1 \text{ kcal mol}^{-1}$ for HCl elimination from **18b'**. Every step is predicted to be strongly exothermic. Scans of θ indicate that rotamers **17b'** and **18b'** in pathway B are actually favored in both cases. Furthermore, the low-energy barriers associated with transition-state complexes **TS1** and **TS2** lead to formation of the conformers in pathway B that ultimately would produce intermediate **20b**. On the other hand, passage of the HCl-elimination barriers favors the route through **TS3** toward **19b** over the one toward **20b** by more than 4 kcal mol^{-1} . The bulk of the *o*-Br ring substituent clearly interferes with the approach

of the catalytic HCl molecule in the transition-state complex formed from **18b'**. $V(\theta)$ exhibits a barrier to rotation between **18b'** and **18b** that is approximately 11 kcal mol^{-1} smaller than the reaction barrier. This evidence suggests that rotation of the *o*-bromophenyl ring occurs much more rapidly than elimination of HCl. For this reason, a near-equilibrium population of the more reactive **18b** rotamer will be maintained during the course of the reaction. As a result, these AM1 calculations predict that kinetic factors in the **18b'** \rightarrow **19b** step govern the production of the observed *o*-Br substituted atropisomer.

In this mechanism, the kinetics of ring closure are adversely affected by factors related to the entropy of activation because rotational freedom of three single bonds is sacrificed in the formation of the transition-state complexes. As the high entropy of activation in this step slows the overall reaction, it undoubtedly contributes to the lack of observable concentrations of dione intermediates, which appear to react as rapidly as they are formed. Catalysis in the HCl-addition step requires two HCl molecules, and this appears to involve an entropically unfavorable tertiary collision. However, the calculations reveal that the reaction is most likely a binary process involving HCl attack on the stable complex **17**·HCl. A kinetic simulation of the reaction taking into account these entropic factors and scaled AM1 barriers is presented as Supporting Information. The simulation supports the proposed mechanism by providing quantitative estimates of reactant, intermediate, and product concentrations that are consistent with experimental observations.

The conclusions drawn from the *o*-Br case were further examined by performing calculations on the **18** \rightarrow **19** HCl-elimination step in the reaction sequences initiated with the (*R,R*) **7** stereoisomer of other aminonitriles in the series under consideration. The difference in the pyrazinone ratio obtained in the reaction undertaken with **8b** was also investigated. The results of these calculations are summarized in Table 3. In those cases where a dominant atropisomer was observed, the calculations do give a correct prediction based on the difference in the value of ΔH_i^\ddagger (**18** \rightarrow **19**) for the two pathways. The small

Table 3. AM1 Data^a for Stereo-Controlling Step in Synthesis of Atropisomeric Pyrazinones

aminonitrile reactant	$\Delta H_f^{\ddagger b}$		$\Delta H_f^{\ddagger c}$		kinetic preference
	19	20	19	20	
7a	31.6	35.2	31.9	31.2	11a \gg 12a
7b	29.8	34.1	19.9	19.1	11b \gg 12b
8b	35.6	30.1	19.9	19.1	12b \gg 11b
7c	29.6	33.4	7.6	7.2	11c \gg 12c
7d	30.0	33.5	-29.9	-30.6	11d \gg 12d
7e	31.4	31.3	6.1	5.7	11e \sim 12e
7f	34.6	37.8	-136.8	-138.5	11f \gg 12f
7i	29.9	30.0	4.6	4.6	11i \sim 12i
7j	30.5	31.0	32.8	32.4	11j \sim 12j
7k	30.6	30.2	17.7	17.5	11k \sim 12k ^d

^a Energies are expressed in kcal mol⁻¹. ^b ΔH_f^{\ddagger} denotes a calculated barrier for acid-catalyzed elimination of HCl from **18**. As indicated in the two subcolumns, the magnitude of this barrier differs in the reaction pathways leading to products **19** and **20**. The predicted kinetic preference is based on the calculated product ratio given by **11:12** = **19:20** \approx exp($\Delta\Delta H_f^{\ddagger}/RT$) where $\Delta\Delta H_f^{\ddagger} = \Delta H_f^{\ddagger}(\mathbf{20}) - \Delta H_f^{\ddagger}(\mathbf{19})$. ^c ΔH_f^{\ddagger} is the calculated AM1 heat of formation. ^d The calculated torsional barriers about the biaryl bond of **19k** are <9 kcal mol⁻¹, which is in accordance with the observed rotational effects on an NMR time scale.

barrier differences obtained in cases **7e** and **7i–k** are also in accord with the lack of strongly dominant atropisomeric products. In the case of the 1-naphthyl substituent (**7j**), the near equality of the barriers indicates why a 1:1 ratio of enantiomers is found even though racemization of the individual atropisomers is predicted to be very slow. However, the prediction that **11** \gg **12** in the cases involving *o*-Cl (**7c**), *o*-F (**7d**), and *o*-CF₃ (**7f**) is clearly out-of-line with experiment. Apparently, the AM1 procedure exaggerates barrier differences for halogen-substituted molecules, especially F and Cl.

Another factor that must be considered to account for the observed product ratios is the rate of racemization of **19** following reaction. From differences in the lowest barrier of the potential curve $V(\theta)$ separating **19** from **20**, the substituent effect on the calculated half-life for the racemization reaction exhibits the trend *o*-CF₃ > *o*-I > *o*-Br > 1-naphthyl > *o*-CH₃ > *o*-Cl > *o*-F \gg *m*-CH₃ \gg 1-thienyl. The calculated rates suggest that rotational isomerization occurs rapidly under high-temperature reaction conditions when X = *o*-F. In comparison, the rate is 20-fold slower when X = *o*-Cl. The observed partial racemization of **11d** and failure to racemize **11c** under experimental conditions of time and temperature is in qualitative accord with the calculated findings. Racemization of the *o*-F compound alters the ratio in the direction of the thermodynamically favored product **12d**, as observed, regardless of the actual value of $\Delta\Delta H_f^{\ddagger}$.

Conclusion

If the *o*-substituent is large (i.e., iodo or bromo) and/or generates a negative electrostatic potential, an unfavorable interaction may occur in the transition state of the step that controls stereoselectivity, namely, the one leading from **18** to **19/20**. The steric and electronic repulsion associated with the **18** \rightarrow **20** step involves the chlorine atom of the catalytic HCl molecule as it extracts the sp³ hydrogen from the carbon bearing the *ortho*-substituted aromatic ring. Lack of this transition-state repulsion favors the **18** \rightarrow **19** reaction, which leads to the observed atropisomer. With smaller groups and those possessing a significant positive partial charge, this

interaction is reduced or eliminated, and mixtures of products are obtained. This model is consistent with the observed trends in selectivity. The selectivity is apparently based on the steric bulk and partial electronic charge of the *ortho* substituent, both of which impact the energy of the transition-state complex. The electronic nature of the aromatic ring appears to have little if any effect on the observed ratio of atropisomers.

Experimental Section

General Methods. Solvents were the anhydrous grade purchased from Aldrich Chemical Co., Milwaukee, WI and were dispensed using standard syringe techniques. All reagents were used as received unless otherwise stated. All nonaqueous reactions were performed in oven-dried (130 °C for >24 h) glassware under a nitrogen atmosphere unless otherwise stated. ¹H and ¹³C NMR spectra were recorded on a Bruker AC 300 NMR spectrometer; infrared spectra, mass spectra, high-resolution mass spectra, and combustion analyses were performed by the Physical and Analytical Chemistry unit of Upjohn Laboratories.

In the preparation of (*aR,R*)-6-(2- α -chlorophenyl)-3-[(1-phenylethyl)amino]-5-chloro-1-(1-furylmethyl)-2(1*H*)-pyrazinone (4**),** a solution of pyrazinone **1a** (372 mg, 1.05 mmol), (*R*)-(+)- α -methylbenzylamine (0.40 mL, 3.10 mmol), and Et₃N (0.70 mL, 5.02 mmol) in CH₂Cl₂ (5.0 mL) was stirred at ambient temperature. After 72 h, the reaction mixture was diluted with CH₂Cl₂ (50 mL) and washed with 1% aqueous HCl (2 \times 50 mL) and H₂O (50 mL). The CH₂Cl₂ extract was dried (MgSO₄), filtered, and concentrated in vacuo. The residue was purified via flash chromatography on silica (eluent, CHCl₃/hexanes 95:5), which gave a colorless syrup. Recrystallization (EtOAc/hexanes) gave the title compound (457 mg, 99%) as white crystals.

The synthesis of (*R,R*)- α -[(1-phenylethyl)amino]- α -(2-bromophenyl)acetone hydrochloride (7b**)** is representative of the procedure used for the synthesis of aminonitriles **5–8** listed in Table 1. (*R*)- α -Methylbenzylamine hydrochloride (12.17 g, 77.20 mmol) and sodium cyanide (3.79 g, 77.33 mmol) were dissolved in H₂O (80 mL). MeOH (80 mL) and 2-bromobenzaldehyde (9.1 mL, 77.95 mmol) were added, and the mixture was stirred for 16 h. The reaction mixture was diluted with H₂O (ca. 200 mL) and extracted with CH₂Cl₂ (3 \times 100 mL). The combined CH₂Cl₂ extracts were dried (Na₂SO₄), filtered, and concentrated in vacuo to give an off-white solid. ¹H NMR (300 MHz, CDCl₃) of this crude material shows it to be a 4.4:1 mixture of diastereomers. The crude solid was dissolved in Et₂O (ca. 300 mL). The addition of methanolic HCl (40 mL; ca. 2 M) gave **7b** as a white crystalline solid (14.008 g, 52%).

The synthesis of (*S,R*)- α -[(1-phenylethyl)amino]- α -(2-bromophenyl)acetone hydrochloride (6b**)** is representative of the procedure used for the synthesis of **5a,b,d,e,g,h,k** and **6b**. (*S*)- α -Methylbenzylamine hydrochloride (20.25 g, 128.46 mmol) and sodium cyanide (6.60 g, 134.67 mmol) were dissolved in H₂O (130 mL). MeOH (130 mL) and 2-bromobenzaldehyde (15.0 mL, 128.49 mmol) were added, and the mixture was stirred for ca. 16 h. The reaction mixture was diluted with H₂O (ca. 500 mL), and the resulting solid was collected via filtration. It was dissolved in a minimum amount of warm PhCH₃ and concentrated in vacuo to give a yellow oil. Trituration of this material with hexanes gave a white solid which was collected via filtration. ¹H NMR (300 MHz, CDCl₃) of this material shows it to be the free base of **6b**. The filtrate was then concentrated in vacuo to give a yellow oil. ¹H NMR (300 MHz, CDCl₃) shows this material to be a 5:1 mixture of **6b** and **5b**. The oil was taken up in Et₂O (ca. 100 mL). The addition of methanolic HCl (10 mL, ca. 2 M) gave **6b** as a white crystalline solid (6.614 g, 15%).

The synthesis of (*aS,S*)-6-(2- α -iodophenyl)-3,5-dichloro-1-(1-phenylethyl)-2(1*H*)-pyrazinone (9a**)** is representative of the cyclization process using chlorobenzene as the solvent.

Aminonitrile **5a** (10.145 g, 28.01 mmol) was added to a solution of oxalyl chloride (7.33 mL, 84.02 mmol) in chlorobenzene (140 mL), and the resulting solution was heated at 70 °C for 14 h. The reaction was cooled to room temperature and concentrated in vacuo, and the resulting residue was purified by silica gel flash chromatography (CHCl₃) to afford 7.515 g (57%) of pure **9a**. An alternate procedure which offered improved yields follows. A heavy-walled glass tube was charged with the aminonitrile hydrochloride **5a** (402 mg, 1.01 mmol), (COCl)₂ (0.30 mL, 3.4 mmol), and PhCH₃ (5 mL). The tube was sealed and the reaction mixture was heated (bath temp 70–75 °C) for 23 h. Upon cooling to ambient temperature, the reaction mixture was concentrated in vacuo, and the residue was purified via flash chromatography on silica (eluant CHCl₃). Recrystallization (EtOAc/hexanes) gave **9a** as a white crystalline solid (271 mg, 60%).

Computational Methods. AM1 calculations were performed at the Hartree–Fock level using the MOPAC 6.0 program.¹⁹ Computation of the potential-energy function, V(P), corresponding to rotation of the substituted phenyl ring, was

carried out by scanning P in 15° increments while allowing all other angles in the molecule to relax. In locating stationary points on the potential-energy surface of each reaction, all degrees of freedom were relaxed until the gradient norm fell below 3.0. Transition-state complexes were established by diagonalizing the calculated Hessian matrix and checking for a single negative eigenvalue.²⁰

Supporting Information Available: X-ray crystallographic structures of **4**, **11a**, and **12a** (including tables of X-ray crystallographic data; spectroscopic and elemental analyses of the compounds synthesized in the course of the study; and simulation of the reaction kinetics in the system **15b** + HCl → ... → **19b** using data from the AM1 calculations and absolute reaction rate theory to estimate rate constants (41 pages). This material is contained in libraries on microfiche, immediately follows this article in the microfilm version of the journal, and can be ordered from the ACS; see any current masthead page for ordering information.

JO9811930

(19) Stewart, J. J. P. *J. Comput. Aided Mol. Des.* **1990**, *4*, 1.

(20) McIver, J. W.; Kormornicki, A. *J. Am. Chem. Soc.* **1972**, *94*, 2980.